

# Sirt1 promotes fat mobilization in white adipocytes by repressing PPAR- $\gamma$

Frédéric Picard<sup>1</sup>, Martin Kurtev<sup>1</sup>, Namjin Chung<sup>1</sup>, Acharawan Topark-Ngarm<sup>2</sup>, Thanaset Senawong<sup>2</sup>, Rita Machado de Oliveira<sup>1,3</sup>, Mark Leid<sup>2</sup>, Michael W. McBurney<sup>4</sup> & Leonard Guarente<sup>1</sup>

<sup>1</sup>Department of Biology, Massachusetts Institute of Technology, Cambridge, Massachusetts 02139, USA

<sup>2</sup>Laboratory of Molecular Pharmacology, Department of Pharmaceutical Sciences, College of Pharmacy and Environmental Health Science Center, Oregon State University, Corvallis, Oregon 97331-3507, USA

<sup>3</sup>Graduate Program in Basic and Applied Biology, ICBAS, University of Porto, 4099-003, Portugal

<sup>4</sup>Ottawa Regional Cancer Centre and Department of Medicine, University of Ottawa, Ontario K1H 1C4, Canada

**Calorie restriction extends lifespan in organisms ranging from yeast to mammals<sup>1</sup>. In yeast, the *SIR2* gene mediates the life-extending effects of calorie restriction<sup>2</sup>. Here we show that the mammalian *SIR2* orthologue, *Sirt1* (sirtuin 1), activates a critical component of calorie restriction in mammals; that is, fat mobilization in white adipocytes. Upon food withdrawal *Sirt1* protein binds to and represses genes controlled by the fat regulator PPAR- $\gamma$  (peroxisome proliferator-activated receptor- $\gamma$ ), including genes mediating fat storage. *Sirt1* represses PPAR- $\gamma$  by docking with its cofactors NCoR (nuclear receptor co-repressor) and SMRT (silencing mediator of retinoid and thyroid hormone receptors). Mobilization of fatty acids from white adipocytes upon fasting is compromised in *Sirt1*<sup>+/-</sup> mice. Repression of PPAR- $\gamma$  by *Sirt1* is also evident in 3T3-L1 adipocytes, where overexpression of *Sirt1* attenuates adipogenesis, and RNA interference of *Sirt1* enhances it. In differentiated fat cells, upregulation of *Sirt1* triggers lipolysis and loss of fat. As a reduction in fat is sufficient to extend murine lifespan<sup>3</sup>, our results provide a possible molecular pathway connecting calorie restriction to life extension in mammals.**

Calorie restriction is the first regimen shown to extend mammalian lifespan. Calorie restriction induces a shedding of body fat from white adipose tissue (WAT), a decrease in body temperature and an increase in insulin sensitivity<sup>4</sup>. It has been suggested that calorie restriction functions in a passive way by lowering oxidative and other damage, thereby resulting in a longer lifespan. However, studies in yeast suggest that calorie restriction is a highly regulated response that requires a sensing step followed by the execution of a programme to extend lifespan<sup>5</sup>. The regulatory gene that mediates this programme is *SIR2*, which promotes survival in yeast<sup>6</sup>, *Caenorhabditis elegans*<sup>7</sup> and, perhaps, higher eukaryotes in response to food scarcity. *SIR2* is well suited for this function because it encodes an NAD-dependent protein deacetylase<sup>1</sup>, enabling it to monitor cellular metabolism and exert corresponding effects on gene expression.

WAT seems to be a primary factor in longevity, as mice engineered to have reduced levels of it live longer<sup>3</sup>. This effect on lifespan may result from changes in hormones that are normally secreted from WAT in proportion to fat mass. Thus, we evaluated whether the mammalian *Sir2* orthologue, *Sirt1*, senses nutrient availability in WAT and mediates corresponding effects on fat accumulation. To probe whether *Sirt1* may actually modulate adipogenesis, we used mouse 3T3-L1 fibroblasts as an *in vitro* model<sup>8</sup>. Adipogenesis in these cells is promoted by the nuclear receptor PPAR- $\gamma$ <sup>9</sup>. Upon induction of adipogenesis by insulin, dexamethasone and isobutyl-

methylxanthine, we observed that *Sirt1* protein levels increased and peaked at day 5 after hormonal stimulation (Fig. 1a). *Sirt1* expression in 3T3-L1 cells was then modified through retroviral infection with either pBABE-*Sirt1* or pSUPER-*Sirt1* RNA interference (RNAi) for overexpression (tenfold) or downregulation (sevenfold) of the *Sirt1* gene, respectively (Fig. 1b). 3T3-L1 cells undergo one or two mitotic divisions after induction as a prelude to terminal differentiation<sup>9,10</sup>. This occurred normally in cells that overexpressed or underexpressed *Sirt1* as evaluated by 5-bromo-deoxyuridine (BrdU) incorporation (data not shown). However, compared with cells infected with the control vector, stable 3T3-L1 cells overexpressing *Sirt1* accumulated much less fat as determined by Oil red O staining after 7 days of differentiation (Fig. 1c) or direct measurement of intracellular triglyceride content (Fig. 1d). In contrast, downregulation of *Sirt1* expression resulted in a significant increase in triglyceride accumulation after differentiation (Fig. 1c, d). These results indicate that *Sirt1* acts a negative modulator of adipogenesis in the 3T3-L1 model.

Insulin/insulin-like growth factor (IGF)-1 signalling helps to regulate adipogenesis<sup>11</sup>, and this pathway determines lifespan in nematode worms<sup>12</sup>. To evaluate the possible interaction of *Sirt1* with the insulin/IGF-1 signalling cascade in adipocytes, we differentiated virally transduced 3T3-L1 cells in the absence of insulin but with rosiglitazone, a very potent, selective PPAR- $\gamma$  agonist that acts downstream of the insulin pathway. Although rosiglitazone treatment promoted adipogenesis to a greater extent than the regular differentiation cocktail (Fig. 1c), it did not alter the phenotypes of cells with increased or decreased levels of *Sirt1* (Fig. 1c), suggesting that *Sirt1* affects regulators that act downstream of insulin/IGF-1 signalling.

Differentiation of 3T3-L1 fibroblasts increases levels of the transcription factor C/EBP- $\delta$ , which stimulates the expression of PPAR- $\gamma$  and C/EBP- $\alpha$ <sup>10</sup>. PPAR- $\gamma$  induces expression of target genes, such as the fatty-acid-binding protein aP2 (also known as adipose tissue-specific FABP)<sup>13</sup>. Moreover, PPAR- $\gamma$  can maintain expression of itself, perhaps by binding to PPAR- $\gamma$  sites in the promoter of the PPAR- $\gamma$  gene (*Pparg*)<sup>9,14</sup>. To gain an insight into the mechanisms by which *Sirt1* represses fat accretion, we measured protein and messenger RNA expression of key factors in the transcriptional programme in the different virus-infected 3T3-L1 adipocytes. We observed a reduction in C/EBP- $\alpha$ , C/EBP- $\delta$  and aP2 mRNA, but not C/EBP- $\beta$ , upon *Sirt1* overexpression (Fig. 1e). A reduction in PPAR- $\gamma$  and C/EBP- $\alpha$  was also observed by western blotting (Fig. 1f). In contrast, cells in which *Sirt1* had been downregulated showed higher levels of PPAR- $\gamma$ , C/EBP- $\delta$ , C/EBP- $\alpha$  and aP2 (Fig. 1e, f). These findings are consistent with the model that *Sirt1* functions as a repressor of genes that drive white adipocyte differentiation and fat storage.

The above experiments do not address whether *Sirt1* regulates fat accumulation in fully differentiated adipocytes. Thus, we fully differentiated 3T3-L1 cells and subsequently (12 days after induction) applied the *Sirt1* activator resveratrol<sup>15</sup> over a wide range of concentrations (Fig. 2a). After staining the cells for fat content, a strong reduction in fat was observed at 50 and 100  $\mu$ M resveratrol. The loss of fat was due to activation of *Sirt1*, because there was no drug-mediated fat reduction in cells in which *Sirt1* levels were knocked down (Fig. 2b). To validate further these visual results, we measured triglyceride content and free fatty acid (FFA) release in these cells. Triglyceride content was reduced and release of FFA was stimulated by resveratrol in the control cells, but not in the *Sirt1* knockdown cells (Fig. 2c). These findings strongly suggest that upregulation of *Sirt1* stimulates fat mobilization in fully differentiated 3T3-L1 adipocytes.

To determine whether *Sirt1* stimulates fat mobilization in bona fide adipocytes, we cultured primary rat white adipocytes and activated fat mobilization with the known  $\beta$ -adrenergic inducer adrenalin. Addition of resveratrol greatly stimulated the release of FFA triggered by adrenalin (Fig. 2d), consistent with the findings in

the 3T3-L1 cells. In a converse experiment using these rat adipocytes, we addressed whether inhibition of Sirt1 would blunt the mobilization of fat by adrenalin. Addition of the known Sirt1 inhibitor nicotinamide<sup>16</sup> indeed reduced the release of FFA triggered by adrenalin (Fig. 2e). The above findings indicate that Sirt1 not only represses the differentiation programme of adipocytes, but also activates the mobilization of fat in fully differentiated cells.

Sirt1 is an NAD-dependent deacetylase that can repress activity of p53 (ref. 1) and forkhead proteins<sup>17,18</sup>. Repression of adipogenesis and fat retention in 3T3-L1 cells by Sirt1 might be explained by inhibition of another transcription factor, PPAR- $\gamma$ , as its activity is crucial for differentiation and maintenance of adipocytes<sup>9,14,19</sup>. Thus, we determined by chromatin immunoprecipitation (ChIP)

assays whether Sirt1 binds to PPAR- $\gamma$  sites in the promoters of the *aP2* and *Pparg* genes. In 3T3-L1 cells, Sirt1 and PPAR- $\gamma$  were both bound to similar promoter regions of *aP2* and *Pparg* (Fig. 3a). The interaction of Sirt1 with both promoter sequences was stronger in Sirt1-overexpressing cells and was lost in Sirt1 knockdown cells (Fig. 3a). Binding of Sirt1 to a control DNA region 2.5 kilobases (kb) upstream of the PPAR- $\gamma$  site near *Pparg* was not observed (data not shown). Furthermore, luciferase reporter assays showed that Sirt1 repressed transactivation by PPAR- $\gamma$  (Fig. 3b). These findings indicate that Sirt1 and PPAR- $\gamma$  bind to the same DNA sequences and suggest that Sirt1 is a co-repressor of PPAR- $\gamma$ .

To gain further evidence that Sirt1 is a PPAR- $\gamma$  co-repressor, we next determined whether the two proteins interact. Sirt1 was

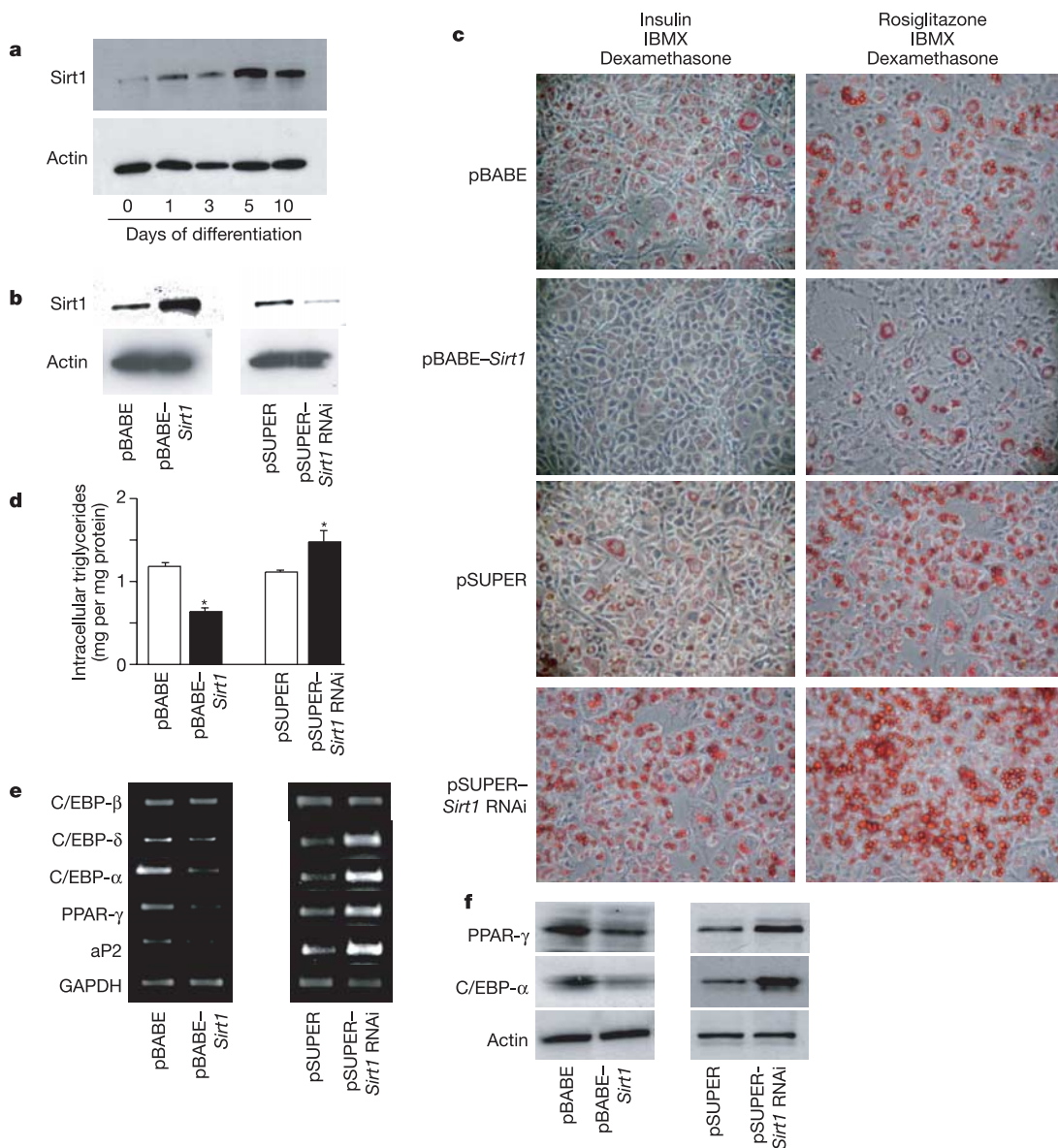


**Figure 1** Sirt1 regulates adipogenesis and triglyceride accumulation in 3T3-L1 cells. **a**, Time course of Sirt1 protein expression on a western blot in 3T3-L1 cells upon induction of adipogenesis. **b**, Sirt1 protein levels in 3T3-L1 cells infected with control pBABE or pSUPER retroviral vectors or with pBABE-Sirt1 or pSUPER-Sirt1 RNAi vectors for overexpression or downregulation of Sirt1, respectively. **c**, Oil red O staining for triglycerides in infected 3T3-L1 cells differentiated for 7 days with IBMX and dexamethasone plus either insulin or rosiglitazone. **d**, Intracellular triglyceride levels in infected 3T3-L1 cells differentiated for 7 days with insulin, IBMX and dexamethasone.

Data shown are means  $\pm$  s.e.m. and were obtained from two independent experiments carried out in triplicate. Asterisk indicates a statistical difference from respective control ( $P < 0.05$ ). **e**, **f**, 3T3-L1 cells were infected and differentiated as in **d**. Protein and total RNA were extracted at day 7. **e**, Reverse transcription and PCRs were on complementary DNAs with gene-specific primers. One microgram of total RNA was used in each case. **f**, Protein levels of PPAR- $\gamma$  and C/EBP- $\alpha$  in total cell extracts measured by western blotting. GAPDH and actin levels are shown as loading controls.

detected in PPAR- $\gamma$  immunoprecipitates from differentiated 3T3-L1 adipocytes (Fig. 3c). The PPAR- $\gamma$  cofactor NCoR<sup>20</sup> was also co-immunoprecipitated by anti-Sirt1 antiserum but not by pre-immune serum (Fig. 3d). Glutathione S-transferase (GST) pull-down experiments revealed that two NCoR fragments interact with Sirt1: repression domain 1 (RD1) and the CBF/Su(H) interaction domain (Fig. 3e). Reciprocally, NCoR RD1 was found to interact with the amino-terminal region of Sirt1 (amino acids 1–214, GST-Sirt1(Nt); Fig. 3f), and the CBF1/Su(H) interaction domain of NCoR interacted with the homology domain of Sirt1 (amino acids 214–541, GST-Sirt1(SHD); Fig. 3f). In analogous experiments, GST pull-down assays revealed an interaction between the Sirt1 homology domain and SMRT (Fig. 3g).

The interaction between Sirt1 and NCoR (and SMRT) suggests that Sirt1 represses PPAR- $\gamma$  activity by docking with the cofactors. Consistent with this, ChIP assays revealed that NCoR also binds to known PPAR- $\gamma$  sites of promoters of adipogenic genes (Fig. 4h). To test the possibility that Sirt1 functionally represses PPAR- $\gamma$  by means of NCoR, we infected Sirt1-overexpressing 3T3-L1 fibroblasts with an NCoR RNAi virus. Western blots showed that doubly infected cells overexpressed Sirt1 and underexpressed NCoR (not shown). As expected, overexpression of Sirt1 in the absence of the NCoR RNAi virus reduced fat accretion (Fig. 4i). In contrast, this reduction was largely prevented on simultaneous treatment with NCoR RNAi (Fig. 4i), demonstrating that NCoR is required for repression of fat accumulation by Sirt1.

To test for a role of Sirt1 in fat mobilization *in vivo*, we first determined whether Sirt1 was expressed in WAT in mice. Sirt1 was found in all white adipose depots examined, with no notable distribution differences (Fig. 4a). Next, to probe for an *in vivo* function, we used mice with germline mutations in the *Sirt1* gene. Unfortunately, the total absence of Sirt1 in mice (*Sirt1*<sup>-/-</sup>) results in a high degree of post-natal lethality and other severe phenotypes, precluding their use in this study<sup>21</sup>. Therefore, we compared wild type to *Sirt1*<sup>+/-</sup> mice, which are phenotypically normal. No significant differences in epididymal WAT mass were observed between the wild type and heterozygous cohorts (Fig. 4b). As yeast Sir2 is important during calorie restriction, we assayed by ChIP the recruitment of Sirt1 to PPAR- $\gamma$ -binding sites in the aP2 and PPAR- $\gamma$  promoters in WAT of mice that were either fed or fasted. In mice fed *ad libitum*, Sirt1 was not bound to aP2 or PPAR- $\gamma$  promoter sequences (Fig. 4c). However, Sirt1 was bound to these sequences after overnight food deprivation, showing that Sirt1 is recruited to PPAR- $\gamma$  DNA-binding sites upon fasting.

As a test of the effect of Sirt1 on fatty acid mobilization in adipocytes, we next addressed whether fatty acid release from WAT upon fasting was altered in *Sirt1*<sup>+/-</sup> mice. Heterozygous gene ablation was associated with a 40–45% lowering in circulating FFA levels in the blood after overnight food deprivation compared with wild type (Fig. 4d,  $P < 0.05$ ). To verify that these effects of *Sirt1* genotype were due to differences in fat release from WAT and not reuptake of FFA from the blood by oxidative tissues, we cultured the

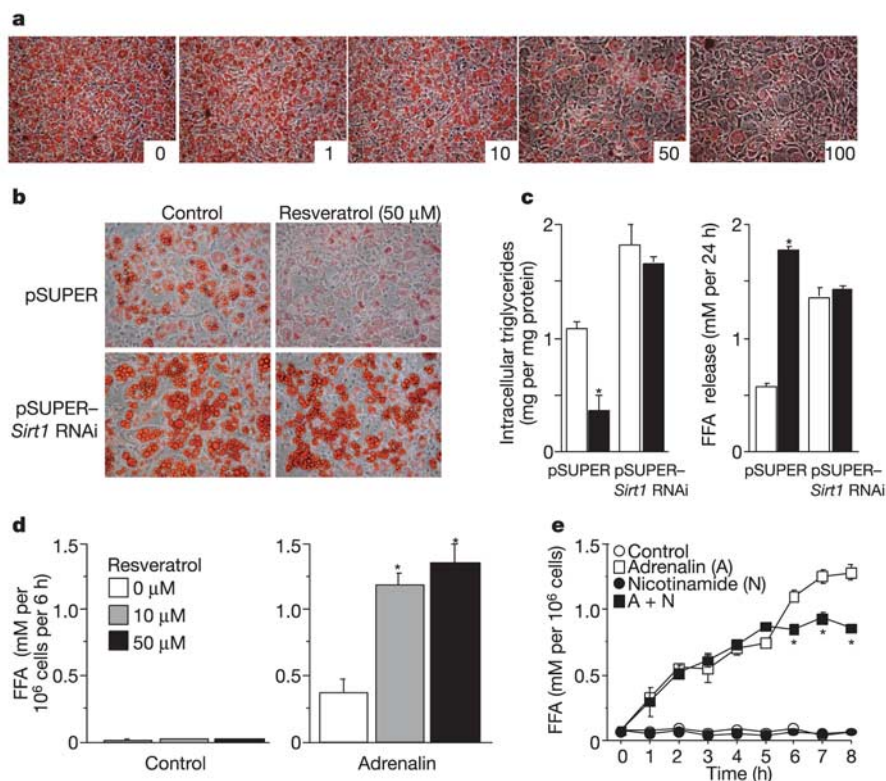


**Figure 2** Activation of Sirt1 by resveratrol decreases fat accumulation in differentiated adipocytes. **a**, Resveratrol addition to 3T3-L1 cells first fully differentiated into adipocytes. At day 12, resveratrol dissolved in DMSO was added in increasing concentrations (1, 10, 50 and 100  $\mu$ M; as indicated) and Oil red O staining was performed 3 days later and compared with cells incubated with DMSO alone (resveratrol 0  $\mu$ M). **b**, **c**, Effect of resveratrol on 3T3-L1 cells infected with the indicated viruses. Cells were differentiated into adipocytes as in Fig. 1d. At day 12, resveratrol (50  $\mu$ M) was added and 3 days later, intracellular triglyceride content was evaluated by Oil red O staining (**b**) and in

cell lysates (**c**). FFA released in the medium during the 3-day incubation period was also measured (**c**). Open bars, control; filled bars, resveratrol. **d**, **e**, Effect of resveratrol on primary adipocytes isolated from rat retroperitoneal WAT. Cells were incubated with or without adrenalin ( $10^{-7}$  and  $10^{-5}$  M for **d** and **e**, respectively) in the presence of Sirt1 activator (resveratrol, **d**) or inhibitor (nicotinamide, **e**). FFA levels released in the medium were measured after 4 h (**d**) or at indicated time points (**e**). Data shown are means  $\pm$  s.e.m. and were obtained from two independent experiments done in triplicate. Asterisk indicates a statistical difference from respective control ( $P < 0.05$ ).



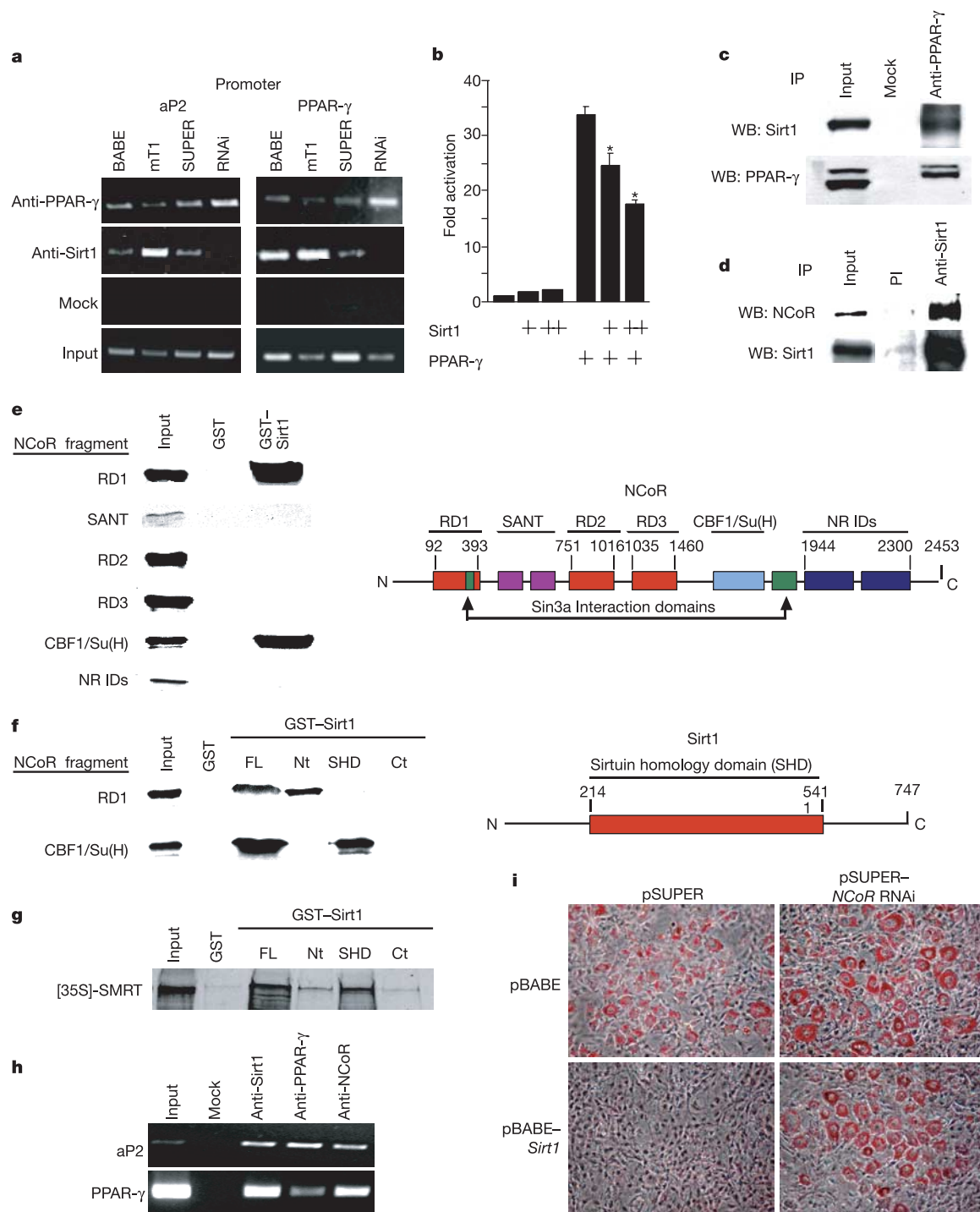


**Figure 3** Sirt1 reduces fat accumulation by repressing PPAR- $\gamma$  activity through Sirt1–NCoR interactions. **a**, ChIP assays on 3T3-L1 cells infected as in Fig. 1c. Cells were differentiated for 7 days and assayed (Methods). **b**, Luciferase assays of 293T cells transfected with mouse PPAR- $\gamma$ 2 and pGL3-PPRE and with increasing concentrations of mouse *Sirt1*. Luciferase was measured 24 h later and was corrected for transfection efficiency. Data represent mean  $\pm$  s.e.m. of triplicate experiments carried out in duplicate. Asterisk indicates a statistical difference ( $P < 0.05$ ). **c**, Co-immunoprecipitation of endogenous PPAR- $\gamma$  and Sirt1 proteins in whole-cell extracts prepared from uninfected differentiated 3T3-L1 adipocytes. **d**, Co-immunoprecipitation of endogenous Sirt1 and NCoR proteins in HEK293 whole-cell extracts using pre-immune (PI) or anti-Sirt1 serum. **e**, Mapping the Sirt1 interaction interface of NCoR. Constructs encoding the indicated NCoR fragments were  $^{35}$ S-methionine-translated and used for GST pull-down experiments as previously

described<sup>30</sup>. A schematic representation of NCoR functional domains is shown on the right. NR IDs, nuclear receptor interaction domains. SANT; Swi3, Ada2, NCoR, TF11B shared motif. **f**, Mapping the NCoR interaction interface of Sirt1. GST pull-down experiments were conducted using radiolabelled NCoR RD1 and CBF1/Su(H) interaction domains and the indicated fragments of Sirt1 fused to GST. A schematic representation of full-length Sirt1 is shown on the right. FL, full length; Nt, N-terminal; Ct, C-terminal. **g**, GST pull-down between the indicated fragments of Sirt1 fused to GST and  $^{35}$ S-methionine-translated SMRT. **h**, ChIP assay in uninfected 3T3-L1 cells differentiated for 7 days with insulin, IBMX and dexamethasone. **i**, RNAi of NCoR. 3T3-L1 cells were infected with either pBABE or pBABE-*Sirt1* and co-infected with either pSUPER or pSUPER-*NCoR* RNAi. Puromycin-selected cells were then differentiated with insulin, IBMX and dexamethasone and stained with Oil red O 7 days later.

same number of white adipocytes from *Sirt1*<sup>+/+</sup> and *Sirt1*<sup>+/-</sup> mice, challenged them with adrenalin, and measured the release of FFA. Again, FFA release was reduced in the *Sirt1*<sup>+/-</sup> cells compared with the *Sirt1*<sup>+/+</sup> cells (Fig. 4e).

Here we show that the mammalian Sir2 orthologue, Sirt1, is activated by food deprivation to trigger fat mobilization in WAT. The pharmacological activation of Sirt1 also elicits the lipolysis of triglycerides and the release of FFA. Because a reduction in fat storage in WAT is a primary way by which calorie restriction extends lifespan in mammals, our results provide a possible mechanism for understanding the regulation of mammalian lifespan by diet. Sirt1 represses WAT by inhibiting the nuclear receptor PPAR- $\gamma$ <sup>13,19</sup>.

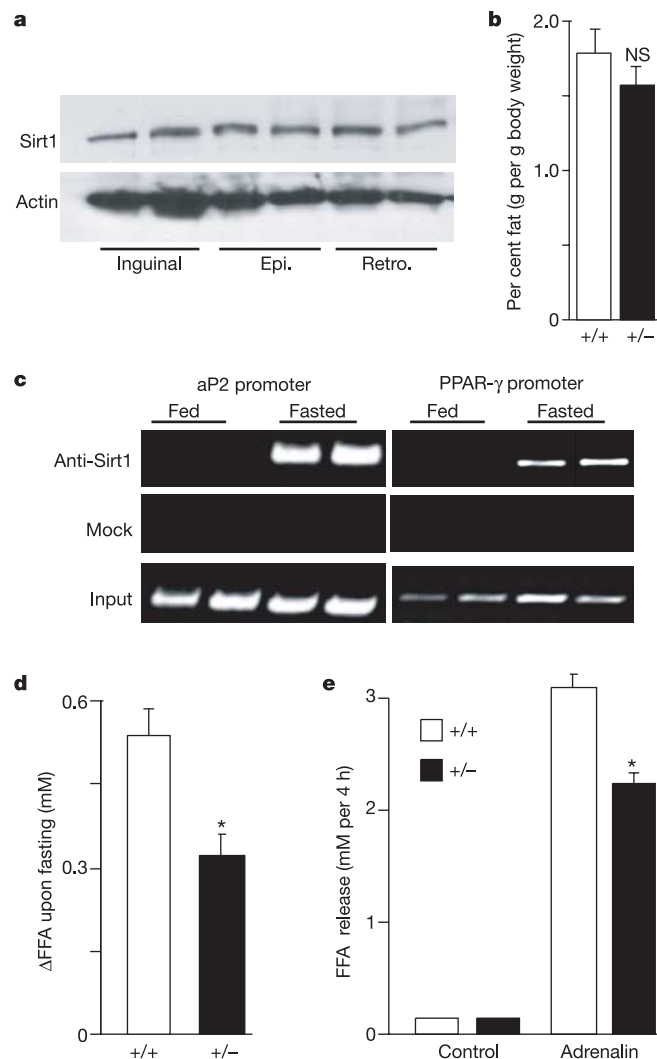


**Figure 4** Sirt1 promotes fat mobilization *in vivo*. **a**, Protein levels of Sirt1 in subcutaneous inguinal and visceral epididymal (Epi.) and retroperitoneal (Retro.) WAT depots in wild-type fed mice. Actin levels are shown as loading controls. Each lane represents an individual mouse. **b**, Weight of epididymal WAT depots in fed *Sirt1*<sup>+/+</sup> and *Sirt1*<sup>+/-</sup> mice. Bars represent mean  $\pm$  s.e.m. ( $n = 10$ – $12$ ; NS, not significant). **c**, *In vivo* ChIP assay in FVB mice either fed or fasted overnight. Each lane represents an individual mouse. Findings represent five independent experiments done in duplicate. **d**, Change in FFA levels in blood from age-matched male *Sirt1*<sup>+/+</sup> and *Sirt1*<sup>+/-</sup> mice between before and after overnight fasting. Bars represent mean  $\pm$  s.e.m. of 27–30 animals. Asterisk indicates a statistical difference from wild-type littermates ( $P < 0.05$ ). **e**, Isolated adipocytes from *Sirt1*<sup>+/+</sup> and *Sirt1*<sup>+/-</sup> mice incubated with or without adrenalin ( $10^{-5}$  M). After 4 h of incubation, FFA released in the medium were measured. Bars represent mean  $\pm$  s.e.m. of triplicate experiments. Asterisk indicates a statistical difference from *Sirt1*<sup>+/+</sup> adipocytes ( $P < 0.05$ ).

Starvation of animals causes Sirt1 to interact with PPAR- $\gamma$  DNA-binding sites and thereby repress target genes that drive fat storage<sup>19</sup>. We do not yet know whether Sirt1 is activated upon fasting by a change in the NAD/NADH ratio, as has been proposed in yeast<sup>22</sup>, or by other metabolic changes. It is also uncertain whether Sirt1 deacetylates PPAR- $\gamma$ , histones at target genes, or both.

The pathway of regulation described here may impact on age-related diseases. The accumulation of WAT during ageing is associated with several adverse complications, such as insulin resistance, type 2 diabetes and atherosclerosis<sup>23</sup>. Given the impact of Sirt1 on PPAR- $\gamma$  activity and because PPAR- $\gamma$  activity helps determine age-related insulin resistance<sup>24</sup>, Sirt1 may have an important role in metabolic diseases and link the effects of food consumption to body fat mass and diseases of ageing. It is likely that calorie restriction exerts other effects on mammals to increase longevity, besides reducing WAT, as longevity in mice with reduced fat is not as great as animals on a long-term calorie restriction regimen. Tissues that metabolize fat and carbohydrate may also be important in delivering some of the benefit of calorie restriction, and it will be of interest to determine whether Sirt1 upregulates metabolism upon food reduction to round out an optimal profile for long life.  $\square$

## Methods

### Animal experimentation

Wild-type FVB male age-matched (12–16 weeks old) mice were used for the present studies. *Sirt1*<sup>+/+</sup> and *Sirt1*<sup>+/-</sup> genotypes have been described previously<sup>21</sup>. All mice were housed under controlled temperature ( $25 \pm 1^\circ\text{C}$  (s.d.)) and lighting conditions. Food provided was normal chow. All mice were cared for in accordance with the MIT animal care committee. Blood was collected from the retro-orbital sinus and kept on ice until centrifugation (1,500 g, 15 min at  $4^\circ\text{C}$ ), and the plasma was stored at  $-20^\circ\text{C}$  until analysis. All animals were killed by decapitation. WAT depots were collected, weighed and quickly frozen in liquid nitrogen and stored at  $-70^\circ\text{C}$  until further processing by immunoblotting. Non-esterified free fatty acids were determined by enzymatic assays (Wako Pure Chemical Industries).

### Cell culture, retroviral infection and transfection

3T3-L1, HEK293, 293T and Phoenix cells (ATCC, Rockville, MD) were cultured in Dulbecco's modified Eagle's medium with 10% FCS, and antibiotics. Primary adipocytes from Sprague-Dawley rats were prepared as described previously<sup>25</sup>. Transfections for luciferase assays were done as described<sup>9,13</sup> using pSPORT6-PPAR- $\gamma$ 2, pGL3-PPRE<sup>26</sup> and pcDNA3-Sirt1. Data were corrected for transfection efficiency.

Retroviral infection was performed as described<sup>9</sup>. Phoenix cells were transfected with either pBABE, pBABE-Sirt1, pSUPERretro (Oligoengine), pSUPERretro-Sirt1 RNAi (5'-GATGAAGTTGACCTCCTCA-3') or pSUPER-NcoR RNAi (5'-GCTGCATCCAAGGGCCATG-3') using Lipofectamine (Invitrogen). After 48 h of transfection, the medium containing retroviruses was collected, filtered, treated by polybrene ( $1 \mu\text{g ml}^{-1}$ ) and transferred to 3T3-L1 target cells. Infected cells were selected with puromycin ( $2.5 \mu\text{g ml}^{-1}$ ) for 7 days.

To stimulate adipogenesis and accumulation of lipids in cells, medium was supplemented to confluent cells (day 0) with  $2 \mu\text{M}$  insulin or  $10^{-7}$  M rosiglitazone (Alexis Biochemicals), as stated in the text,  $1 \mu\text{M}$  dexamethasone, and  $0.25 \text{ mM}$  isobutylmethylxanthine (IBMX) for 2 days. The cells were then incubated with insulin or  $10^{-7}$  M rosiglitazone, changing the medium every second day. Fat accumulation was visualized by staining of lipids with Oil red O. Intracellular triglyceride levels were measured in cell lysates by an enzymatic method using a reagent kit from Boehringer Mannheim.

### RNA and protein preparation and analysis

Total RNA from cultured cells were extracted (Qiagen) and analysed by semi-quantitative polymerase chain reaction with reverse transcription. GAPDH and 18S RNA levels were determined as a control for loading. Primer sequences have been described elsewhere<sup>19,27</sup>. Proteins from mouse tissues were extracted in a solution of pH 7.4 containing 20 mM HEPES, 250 mM sucrose, 4 mM EDTA, 1% Triton and protease inhibitor cocktail. 3T3-L1 cells were lysed in NET-N buffer (20 mM Tris-HCl, pH 8 containing 150 mM NaCl, 0.5% NP-40, 10% glycerol, 1 mM EDTA and a protease inhibitor cocktail).

### Chromatin immunoprecipitation

For *in vitro* ChIP, infected 3T3-L1 cells were differentiated as mentioned above. For *in vivo* ChIP, epididymal WAT was dissected, minced and fixed overnight in PBS containing 1% formaldehyde and protease inhibitor cocktail. Tissues were then rinsed five times in PBS. Further ChIP assays were performed as described previously<sup>28</sup>, using 1:200 antibody dilutions to immunoprecipitate DNA-protein complexes. DNA was then purified using Qiagen PCR purification kit and PCR reaction was performed using primers for aP2 (5'-AAATTCAGAAAGTAACACATTATT-3'; 5'-ATGCCTGACCATGTGA-3') and PPAR- $\gamma$  proximal (amplifying a region at 0.3 kb upstream of ATG: 5'-GAGCAAGGTCTTCATCATTACG-3'; 5'-CCCCTGGAGCTGGAGTTAC-3') and distal

(amplifying a region at 2.8 kb upstream of ATG: 5'-CTCTCCACCTCGCCATAC-3'; 5'-TTGCCAGAGAGCCAGTGACA-3') promoters.

## Pull-down and co-immunoprecipitation assays

Differentiated 3T3-L1 or HEK293 cells were lysed in NET-N buffer by agitation at 4 °C for 30 min. After a brief sonication, lysates were cleared by centrifugation and immunoprecipitated. Antibodies used were anti-Sirt1 (Upstate), anti-NCoR (Upstate), anti-PPAR- $\gamma$  (SantaCruz), anti-C/EBP- $\alpha$  (SantaCruz) and anti-Sirt1 antiserum<sup>29</sup> or preimmune serum. Immunoprecipitates were then analysed by immunoblotting. Equivalent amounts of GST or GST-Sirt1 fusion proteins were bound to glutathione-Sepharose (Pharmacia) and incubated with <sup>35</sup>S-methionine-labelled NCoR or SMRT fragments prepared using TNT transcription-translation system (Promega). The reactions were washed five times with binding buffer (10 mM Na-HEPES containing 10% glycerol, 1 mM EDTA, 1 mM DTT, 150 mM NaCl and 0.05% NP-40) and bound proteins were eluted and resolved on denaturing SDS-polyacrylamide gel electrophoresis gels for analysis by autoradiography.

## Statistical analysis

The main and interactive effects were analysed by analysis of variance (ANOVA) factorial or repeated measures when appropriate. When justified by the ANOVA analysis, differences between individual group means were analysed by Fisher's PLSD test. Differences were considered statistically significant at  $P < 0.05$ .

Received 28 January; accepted 16 April 2004; doi:10.1038/nature02583.

Published online 2 June 2004.

- Koubova, J. & Guarente, L. How does calorie restriction work? *Genes Dev.* **17**, 313–321 (2003).
- Lin, S. J., Defossez, P. A. & Guarente, L. Requirement of NAD and SIR2 for life-span extension by calorie restriction in *Saccharomyces cerevisiae*. *Science* **289**, 2126–2128 (2000).
- Blüher, M., Kahn, B. B. & Kahn, C. R. Extended longevity in mice lacking the insulin receptor in adipose tissue. *Science* **299**, 572–574 (2003).
- Weindruch, R. & Walford, R. L. *The Retardation of Aging and Disease by Dietary Restriction* (C. C. Thomas, Springfield, Illinois, 1988).
- Lin, S. J. *et al.* Calorie restriction extends *Saccharomyces cerevisiae* lifespan by increasing respiration. *Nature* **418**, 344–348 (2002).
- Kaeberlein, M., McVey, M. & Guarente, L. The SIR2/3/4 complex and SIR2 alone promote longevity in *Saccharomyces cerevisiae* by two different mechanisms. *Genes Dev.* **13**, 2570–2580 (1999).
- Tissenbaum, H. A. & Guarente, L. Increased dosage of a sir-2 gene extends lifespan in *Caenorhabditis elegans*. *Nature* **410**, 227–230 (2001).
- Green, H. & Kehinde, O. Sublines of mouse 3T3 cells that accumulate lipid. *Cell* **1**, 113–116 (1974).
- Tontonoz, P., Hu, E. & Spiegelman, B. M. Stimulation of adipogenesis in fibroblasts by PPAR $\gamma$ 2, a lipid-activated transcription factor. *Cell* **79**, 1147–1156 (1994).
- Rosen, E. D. & Spiegelman, B. M. Molecular regulation of adipogenesis. *Annu. Rev. Cell Dev. Biol.* **16**, 145–171 (2000).
- Nakae, J. *et al.* The forkhead transcription factor Foxo1 regulates adipocyte differentiation. *Dev. Cell* **4**, 119–129 (2003).
- Kenyon, C. A conserved regulatory system for aging. *Cell* **105**, 165–168 (2001).
- Tontonoz, P., Hu, E., Graves, R. A., Budavari, A. I. & Spiegelman, B. M. mPPAR $\gamma$ 2: tissue-specific regulator of an adipocyte enhancer. *Genes Dev.* **8**, 1224–1234 (1994).
- Ren, D., Collingwood, T. N., Rebar, E. J., Wolfe, A. P. & Camp, H. S. PPAR $\gamma$  knockdown by engineered transcription factors: exogenous PPAR $\gamma$ 2 but not PPAR $\gamma$ 1 reactivates adipogenesis. *Genes Dev.* **16**, 27–32 (2002).
- Howitz, K. T. *et al.* Small molecule activators of sirtuins extend *Saccharomyces cerevisiae* lifespan. *Nature* **425**, 191–196 (2003).
- Fulco, M. *et al.* Sir2 regulates skeletal muscle differentiation as a potential sensor of the redox state. *Mol. Cell* **12**, 51–62 (2003).
- Motta, M. C. *et al.* Mammalian SIRT1 represses forkhead transcription factors. *Cell* **116**, 551–563 (2004).
- Brunet, A. *et al.* Stress-dependent regulation of FOXO transcription factors by the SIRT1 deacetylase. *Science* **303**, 2011–2015 (2004).
- Tamori, Y., Masugi, J., Nishino, N. & Kasuga, M. Role of peroxisome proliferator-activated receptor- $\gamma$  in maintenance of the characteristics of mature 3T3-L1 adipocytes. *Diabetes* **51**, 2045–2055 (2002).
- Dowell, P. *et al.* Identification of nuclear receptor corepressor as a peroxisome proliferator-activated receptor alpha interacting protein. *J. Biol. Chem.* **274**, 15901–15907 (1999).
- McBurney, M. W. *et al.* The mammalian SIR2 $\alpha$  protein has a role in embryogenesis and gametogenesis. *Mol. Cell. Biol.* **23**, 38–54 (2003).
- Lin, S.-J., Ford, E., Haigis, M., Liszt, G. & Guarente, L. Calorie restriction extends yeast life span by lowering the level of NADH. *Genes Dev.* **18**, 12–16 (2004).
- Gabriely, I. & Barzilai, N. The role of fat cell derived peptides in age-related metabolic alterations. *Mech. Ageing Dev.* **122**, 1565–1576 (2001).
- Miles, P. D., Barak, Y., Evans, R. M. & Olefsky, J. M. Effect of heterozygous PPAR $\gamma$  deficiency and TZD treatment on insulin resistance associated with age and high-fat feeding. *Am. J. Physiol.* **284**, E618–E626 (2003).
- Marette, A., Deshaies, Y., Collet, A. J., Tulp, O. & Bukowiecki, L. J. Major thermogenic defect associated with insulin resistance in brown adipose tissue of obese diabetic SHR/N-cp rats. *Am. J. Physiol.* **261**, E204–E213 (1991).
- Forman, B. M. *et al.* 15-Deoxy- $\Delta$ 12,14 prostaglandin J2 is a ligand for the adipocyte determination factor PPAR $\gamma$ . *Cell* **83**, 803–812 (1995).
- Le Lay, S., Lefrère, I., Trautwein, C., Dugail, I. & Krief, S. Insulin and sterol-regulatory element-binding protein-1c (SREBP-1c) regulation of gene expression in 3T3-L1 adipocytes. *J. Biol. Chem.* **277**, 35625–35634 (2002).
- Fajas, L. *et al.* E2Fs regulate adipocyte differentiation. *Dev. Cell* **3**, 39–49 (2002).
- Langley, E. *et al.* Human SIR2 deacetylates p53 and antagonizes PML/p53-induced cellular senescence. *EMBO J.* **21**, 2383–2396 (2002).
- Dowell, P., Peterson, V. J., Zabriskie, M. & Leid, M. Ligand-induced peroxisome proliferator-activated receptor alpha conformational change. *J. Biol. Chem.* **272**, 2013–2020 (1997).

**Acknowledgements** We thank B. Spiegelman for the gift of constructs and for discussion; T. Kouzarides and T. Heinzel for Sirt1 and NCoR constructs, respectively; and R. Frye for the anti-Sirt1 antiserum. The Guarente laboratory was supported by grants from the NIH, the Ellison Medical Foundation, and the Howard and Linda Stern Fund. Studies in the Leid laboratory were supported by grants from the National Institutes of Health and by a NIEHS Center grant to the Oregon State University Environmental Health Sciences Center. T.S. was supported by a graduate fellowship from the Royal Thai Government. R.M.O. is supported by the Portuguese Foundation for Science and Technology. M.K. is a Howard Hughes undergraduate research fellow. F.P. was supported in part by a postdoctoral fellowship from the Canadian Institutes of Health Research.

**Competing interests statement** The authors declare competing financial interests: details accompany the paper on [www.nature.com/nature](http://www.nature.com/nature).

**Correspondence** and requests for materials should be addressed to L.G. (leng@mit.edu).

## Plant retinoblastoma homologues control nuclear proliferation in the female gametophyte

Chantal Ebel, Luisa Mariconti & Wilhelm Grissem

Institute of Plant Sciences, Swiss Federal Institute of Technology, ETH Zürich, Universitätstrasse 2, CH-8092 Zürich, Switzerland

Haploid spores of plants divide mitotically to form multicellular gametophytes. The female spore (megaspore) of most flowering plants develops by means of a well-defined programme into the mature megagametophyte consisting of the egg apparatus and a central cell<sup>1,2</sup>. We investigated the role of the *Arabidopsis* retinoblastoma<sup>3,4</sup> protein homologue and its function as a negative regulator of cell proliferation during megagametophyte development. Here we show that three mutant alleles of the gene for the *Arabidopsis* retinoblastoma-related protein, *RBR1* (ref. 4), are gametophytic lethal. In heterozygous plants 50% of the ovules are aborted when the mutant allele is maternally inherited. The mature unfertilized mutant megagametophyte fails to arrest mitosis and undergoes excessive nuclear proliferation in the embryo sac. Supernumerary nuclei are present at the micropylar end of the megagametophyte, which develops into the egg apparatus and central cell. The central cell nucleus, which gives rise to the endosperm after fertilization, initiates autonomous endosperm development reminiscent of *fertilization-independent seed (fis)* mutants<sup>5</sup>. Thus, *RBR1* has a novel and previously unrecognized function in cell cycle control during gametogenesis and in the repression of autonomous endosperm development.

During female gametophyte development in *Arabidopsis*, the haploid nucleus of one of the four meiotic spores undergoes three consecutive mitotic divisions. This is followed by cellularization, in which the eight nuclei are assembled into a seven-cell structure comprised of three antipodals, two synergids and the egg cell (egg apparatus), and a binucleate central cell. After degeneration of the three antipodal cells and fusion of the central cell nuclei, the mature female gametophyte (megagametophyte) has four visible nuclei before fertilization<sup>1,2</sup>. Although mutants have been identified that affect megagametophyte development<sup>6</sup>, maize *indeterminate gametophyte1 (ig)* is the only known mutation that fails to arrest mitotic divisions in the mature megagametophyte<sup>7</sup>. In contrast, mitotic division of the central cell nucleus and autonomous endosperm development in the absence of fertilization is common to the *fis*-class of mutants<sup>8–12</sup> that have a gametophytic maternal effect. *FIS*-class genes encode proteins of the polycomb group (PcG), including MEA, FIE, FIS2 and the WD-40 repeat protein MSI1, which control cell proliferation<sup>5,8–12</sup>. In animals and plants, the